Prompt muon contribution to the flux underwater

T. S. Sinegovskaya
Applied Physics Institute, Irkutsk State University, Irkutsk, 664003, Russia

S. I. Sinegovsky
Physics Faculty, Irkutsk State University, Irkutsk, 664003, Russia

(Received 29 September 2000; published 3 April 2001)

We present high energy spectra and zenith-angle distributions of the atmospheric muons computed for the depths of the locations of the underwater neutrino telescopes. We compare the calculations with the data obtained in the Baikal and the AMANDA muon experiments. The prompt muon contribution to the muon flux underwater due to recent perturbative QCD-based models of the charm production is expected to be observable at the depths of the large underwater neutrino telescopes. This appears to be probable even at rather shallow depths (1–2 km), provided the energy threshold for muon detection is raised above ~ 100 TeV.

DOI: 10.1103/PhysRevD.63.096004 PACS number(s): 96.40.Tv, 95.55.Vj, 95.85.Ry

I. INTRODUCTION

A considerable body of literature exists on estimating the contribution to cosmic ray muon fluxes that arises from the decay of charmed hadrons [1–11]. Current data on the high-energy atmospheric muon flux obtained with many surface and underground detectors are too conflicting to provide the means of probing charm production models (see, for example, Ref. [8]).

Both direct and indirect measurements of the atmospheric muon flux at sea level are limited to ~ 70 TeV for the vertical and to ~ 50 TeV for the horizontal. Statistical reliability of these data is still insufficient to evaluate the prompt muon contribution to the high-energy muon flux. Available energies and the accuracy of underground measurements are constrained because of the restricted size of detectors and the uncertainties in the local rock density. Deep-sea installations have substantial advantages just due to large detector volume and homogeneous matter. So it is relevant to discuss the potential of the large underwater neutrino detectors (AMANDA, Baikal), in the context of the prompt muon study, in future high-energy muon experiments.

In this paper, we present calculations on the zenith angle dependence of the high energy underwater muon flux taking into consideration the prompt muon fraction obtained in one of the recent perturbative QCD (PQCD) models of Pasquali *et al.* [9] in which the small-x behavior of the gluon distributions is probed. This PQCD calculation based on Martin-Roberts-Stirling set D$_-$ (MRSD-) [12] and CTEQ3 [13] parton distribution functions (PDF's) includes the next-to-leading order (NLO) corrections to the charm production cross sections.

Perturbative QCD models differ in the PDF sets being employed in the NLO calculations and in the choice of renormalization and factorization scales. A dependence on these quantities of the vertical sea-level prompt lepton fluxes was studied in Refs. [9,11,14]. The predictions of the PQCD model [9] are comparable to those of the earlier quark-gluon string model [15] and the recombination quark-parton one (see [6,8]). The muon spectra underwater obtained with the PQCD models and other types of charm production models, the quark-gluon string model (QGSM) and the recombination quark-parton model (RQPM), were partly discussed in Ref. [10]. Here we would like to focus on variations in the expected underwater muon fluxes caused by distinctions between the PDF's used. In addition, we compare the expected underwater muon flux to the zenith angle distributions measured with the Baikal neutrino telescope [16] and the Antarctic Muon and Neutrino Detector Array (AMANDA) [17].

II. SEA-LEVEL MUON FLUXES

The atmospheric muon energy spectra and zenith angle distributions of the conventional (π,K) muons, and the RQPM and the QGSM contribution, have been computed using the same nuclear cascade model [8,18,19]. Let us glance over its key assumptions.

(i) The all-particle primary spectra and chemical composition are taken according to Ref. [20]. Nuclei of the primary cosmic rays are treated as the composition of free nucleons.

(ii) Feynman scaling is assumed to be valid for hadrons produced in collisions of hadrons with nuclei of the atmosphere.

(iii) The inelastic cross sections σ_{hA}^{inel} for interactions of a hadron h $(=p,n,\pi^{\pm})$ with a nucleus A grow logarithmically with the energy:

$$\sigma_{hA}^{inel}(E_h)=\sigma_{hA}^{0}+\sigma_A \ln(E_h/1\ \text{TeV}).$$

(iv) The hadron production in kaon-nucleus and in charmed hadron-nucleus collisions is neglected.

(v) Charged pion is considered stable in the kinetic stage of the nuclear cascade (not in the stage of muon production, to be sure).

(vi) Three-particle semileptonic kaon decays $K_{\mu 3}$ are taken into account.

The energy spectrum of the conventional muons calculated for the vertical at the sea level can be approximated [8] by the formula

$$\mathcal{D}_{\mu}^{\pi,K}(E_{\mu},0^{\circ})=\begin{cases} A_1(E_{\mu}/E_1)^{-(0.3061+1.2743y-0.263y^2+0.0252y^3)}, & 1\leqslant E_{\mu}\leqslant 927.65 \text{ GeV}, \\ A_2(E_{\mu}/E_1)^{-(1.791+0.304y)}, & 927.65<E_{\mu}\leqslant 1587.8 \text{ GeV}, \\ A_3(E_{\mu}/E_1)^{-3.672}, & 1587.8<E_{\mu}\leqslant 4.1625\times 10^5 \text{ GeV}, \\ A_4(E_{\mu}/E_1)^{-4}, & E_{\mu}>4.1625\times 10^5 \text{ GeV}. \end{cases}$$

Here $E_1=1$ GeV, $y=\log_{10}(E_{\mu}/E_1)$, $A_1=2.95\times 10^{-3}$, $A_2=1.781\times 10^{-2}$, $A_3=14.35$, $A_4=10^3$(cm^{-2} s^{-1} sr^{-1} GeV^{-1}).

The results of the calculations of the muon zenith-angle distributions at sea level are presented in Table I for high energies 1–100 TeV. The differential energy spectra (scaled by E_{μ}^3) of the conventional muons at sea level are shown (solid) in Fig. 1 for the vertical and near horizontal direction together with the data of the Nottingham spectrograph [21] (one point at $E_{\mu}\simeq 1.3$ TeV), the MUTRON spectrometer [22], and indirect measurements [23–28]. Open circles represent the MACRO best fit for the verical direction [28]. (The detailed comparison between the calculated muon energy spectra for different zenith angles and the sea-level experimental data, in particular for large zenith angles, as well as calculations of other authors, is made in Ref. [29].)

Dashed and dotted lines in Fig. 1 correspond to the vertical muon flux including the prompt muon contributions calculated [9] with the CTEQ3 functions (PQCD-2) and the MRSD- set (PQCD-1). Line 1 (dashed) corresponds to the MRSD- set, line 2 (short dotted) corresponds to the CTEQ3 PDF, both with factorization and renormalization scales $\mu_F=2\mu_R=2m_c$, and with the charm quark mass $m_c=1.3$ GeV. As evident from the figure, the PQCD predictions depend strongly on the PDF.

For comparison there are also shown predictions of the charm production model of Volkova, Fulgione, Galeotti, and Saavedra (VFGS) [5] (thin) and the results obtained with the RQPM (dot-dashed) and the QGSM (dotted), both for the vertical direction (lower) and near the horizontal (up). These results enable one to make out the range of prompt muon flux predictions that overspread more than one order of magnitude at $E_{\mu}\sim 1$ PeV. It is interesting to note that old QGSM predictions [6,15] coincide practically with those of the PQCD-2 up to ~ 600 TeV, while the RQPM flux appears to be close to the PQCD-1 one.

As is seen from Fig. 1, at $E_{\mu}\gtrsim 20$ TeV none of the above models but the VFGS is consistent with the data of MSU [23] and Frejus [24]. Conversely, none of the charm production models under discussion contradict the LVD data [25,30]. The VFGS, differing from the others in the extent of optimism, gives the greatest prompt muon flux that is scarcely compatible with the LVD upper limit [30].

The ''crossing energy'' $E_{\mu}^c(\theta)$ (the energy around which the fluxes of conventional and prompt muons become equal) depends on the choice of the PDF set. The vertical crossing energy $E_{\mu}^c(0^{\circ})$ is about 200 TeV for the PQCD-1 model, which is close to the RQPM prediction ($E_{\mu}^c\sim 150$ TeV). The vertical prompt muon flux predicted with the PQCD-2 model becomes dominant over the conventional one at the energies $E_{\mu}\gtrsim 500$ TeV. Therefore in order for the differences between the PQCD models to be found experimentally one needs to measure muon energies above ~ 100–200 TeV.

TABLE I. Ratio $\mathcal{D}_{\mu}^{\pi,K}(E_{\mu},\theta)/\mathcal{D}_{\mu}^{\pi,K}(E_{\mu},0^{\circ})$ of differential energy spectra of the conventional muons at sea level as a function of sec θ.

sec θ	E_{μ} (TeV)						
	1	3	5	10	30	50	100
1.0	1.0	1.0	1.0	1.0	1.0	1.0	1.0
2.0	1.74	1.86	1.90	1.93	1.96	1.96	1.97
3.0	2.28	2.58	2.67	2.75	2.82	2.83	2.84
4.0	2.66	3.12	3.27	3.40	3.52	3.54	3.57
5.0	2.94	3.56	3.76	3.95	4.12	4.15	4.19
10.0	3.53	4.69	5.09	5.50	5.86	5.95	6.01
15.0	3.61	5.00	5.49	5.99	6.45	6.56	6.65
20.0	3.57	5.05	5.58	6.12	6.63	6.75	6.85
40.0	3.31	4.88	5.44	6.02	6.56	6.69	6.79
57.3	3.17	4.74	5.30	5.88	6.41	6.54	6.64

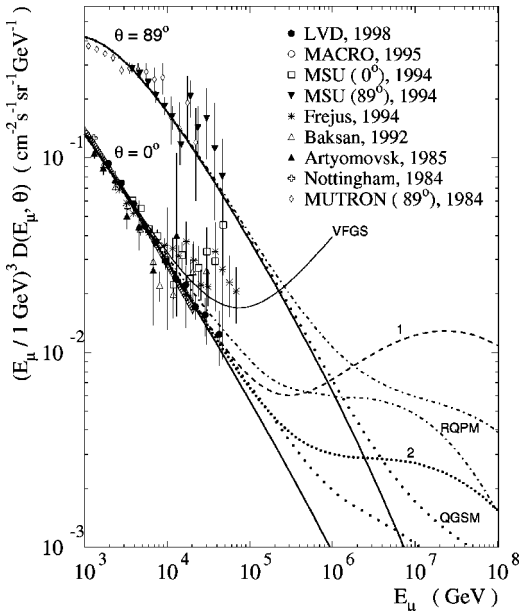

FIG. 1. Sea-level muon fluxes for the vertical and horizontal. The solid lines are for the conventional muons alone. Also shown are the conventional muons plus the prompt muon contribution estimated with several models: the PQCD-1 (dashed) and PQCD-2 (short dotted) for the vertical; the model of Volkova *et al.* (thin) for the vertical; the RQPM (dot-dashed) and QGSM (dotted) for the vertical (lower) and near the horizontal (up).

III. MUON FLUXES UNDERWATER

Muon energy spectra and zenith angle distributions deep underwater are calculated using an analytical method [31] (see also Ref. [8]). By this method one can solve the problem of the muon passing through dense matter for an arbitrary ground-level muon spectrum and real energy dependence of differential cross sections of muon-matter interactions. The collision integral on the right-hand side of the muon transport equation describes the ''discrete'' energy loss of muons due to bremsstrahlung, direct e^+e^- pair production and photonuclear interactions.

In this paper the ionization energy loss and the part of the loss due to e^+e^- pair production with $v<2\times10^{-4}$ (v is the fraction of the energy lost by the muon) is treated as a continuous one: that is, the corresponding item is subtracted from the collision integral and transferred to the left-hand side as a partial derivative with respect to energy of the mean energy loss rate multiplied by the muon flux.

The calculations of the prompt muon fluxes underwater at different zenith angles were performed with the parameterization of the sea-level muon differential spectra (PQCD-1,2) taken from Ref. [9].

Omitting details, we dwell on a factor that may be useful in correcting the underwater muon flux, provided that it is crudely estimated with the continuous energy loss approximation (see Ref. [31]). This factor is the ratio $R_{d/c}$ of the integral muon flux $I_\mu^{\rm disc}(E_\mu,h,\theta)$, computed for discrete (stochastic) muon energy losses, to the flux $I_\mu^{\rm cont}(E_\mu,h,\theta)$ estimated with the continuous loss approximation. In Table II the ratio $R_{d/c}$ is given as a function of the water depth and zenith angle for muon energies above 10 GeV. As is seen the effect of discrete energy loss for the large depth is far from being small: $R_{d/c}$ is about 2 for the depth value of ~10 km w.e. The ratio is slightly affected by zenith-angular dependence of the sea-level muon flux. More precisely, the $R_{d/c}$ depends both on the ''spectral index'' of the muon flux and geometric factor of $\sec\theta$. The former varies weakly with zenith angle while the latter plays more important role in the $R_{d/c}$ defining the thickness of water layer $X=h\sec\theta$ that a muon overpasses (h indicates the vertical depth in km).

TABLE II. Ratio $R_{d/c}=I_\mu^{\rm disc}/I_\mu^{\rm cont}$ at $E_\mu>10$ GeV.

θ	$\sec\theta$	h (km w.e.)			
(degrees)		1	2	3	4
0	1.0	1.02	1.05	1.09	1.15
60	2.0	1.04	1.14	1.31	1.58
70.53	3.0	1.08	1.30	1.74	2.54
75.52	4.0	1.12	1.55	2.53	4.79
78.46	5.0	1.20	1.96	4.07	10.7
80.40	6.0	1.30	2.60	7.21	28.7
81.79	7.0	1.43	3.57	13.8	89.5
82.82	8.0	1.58	5.00	28.7	284
83.62	9.0	1.74	7.10	63.5	769
84.26	10.0	1.92	10.5	151	2320

For water the ratio $R_{d/c}$ as a function of the slant depth X can be approximated with accuracy better than $\sim10\%$ as

$$R_{d/c}(X)=\begin{cases}0.99+0.02X+6.74\times10^{-4}X^3, & 1\leqslant X<12 \text{ km},\\ 1.43+0.054\exp[(X-1.19)/3.64], & 12\leqslant X\leqslant 35 \text{ km}.\end{cases}$$

The effect of the discrete loss increases as the muon energy grows. The energy dependence of the ratio $R_{d/c}$ is adequately illustrated by the following: for the depth of 12 km w.e. $R_{d/c}\simeq2.5$ at $E_\mu=10$ GeV and $R_{d/c}\simeq4.0$ at $E_\mu=1$ TeV.

In Fig. 2 we present a comparison between the expected muon vertical depth-intensity relation in water and the data obtained in underwater experiments (see, for review, Refs. [8] and [16]), including recent measurements in the AMANDA-B4 experiment [17]. The computation was performed with water parameters: $\varrho=1$ g/cm^3, $\langle Z\rangle=7.47$, $\langle A\rangle=14.87$, $\langle Z/A\rangle=0.5525$, $\langle Z^2/A\rangle=3.77$. The muon energy loss per 1 g/cm^2 in ice is considered to be equal that in water but $\varrho_{ice}=0.92$ g/cm^3. The calculations are presented for the muon residual energy (threshold of the detection) $E_\mu\geqslant1$ GeV (solid) and $E_\mu\geqslant20$ GeV (dashed). This difference needs to be considered especially for shallow depth.

Figures 3 and 4 show a comparison of the predicted muon zenith angle distribution (without considering the prompt muon contribution) with the measurements in the neutrino telescopes NT-36 [16] and AMANDA [17].

The line in Fig. 3 presents the calculation for the muon threshold energy $E_\mu=10$ GeV at depth $h=1.15$ km. Our calculation is in reasonable agreement with the measurements of the NT-36 at all but the angle range 80–84°. In Fig. 4, the upper line relates to the flux at the depth $h=1.60$ km w.e. calculated for the muon residual energy $E_\mu\geqslant20$ GeV, the lower one relates to $h=1.68$ km w.e. for the same energy threshold. The difference illustrates the possible effect of an uncertainty in determining the average ''trigger depth'' [17] (relating to the center of gravity of all hit optical modules in the AMANDA-B4 experiment). The computed angle distribution agrees fairly well with the AMANDA-B4 data including zenith angles $\theta>70°$.

The contributions of the (π,K) and prompt muons underwater to zenith angle distribution at $E_\mu>100$ TeV calculated for four values of depths (of 1.15–4 km) are shown in Fig. 5. Here we present the results obtained with the

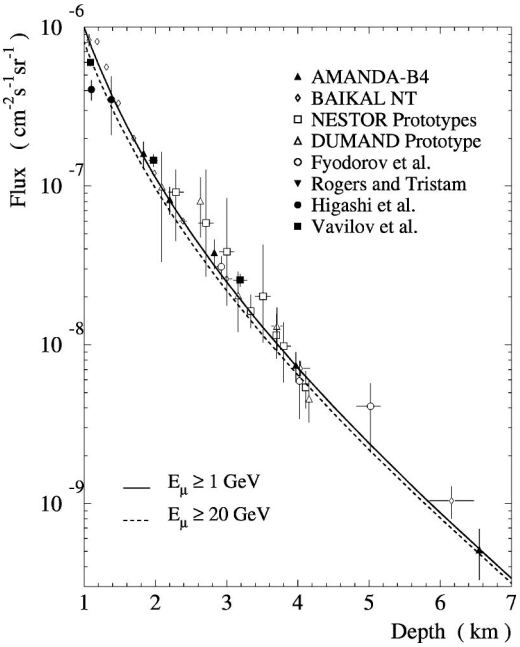

FIG. 2. Vertical muon flux as a function of water depth. The lines correspond to the π,K muons calculated with the muon residual energy above 1 GeV (solid) and above 20 GeV (dashed).

PQCD-1 (dashed) and the PQCD-2 (dotted). It is interesting to note that the dashed line representing the PQCD-1 prompt muon contribution twice intersects the line of the conventional flux at $h=1.15$ km: near the vertical and at $\theta \sim 75°$. This can occur because of the different zenith angle dependence of the conventional muon flux and the prompt muon one. And this means that at a depth of 1.15 km the nearly doubled muon event rate (for $E_\mu > 100$ TeV) would be observed in the 0–75° range, instead of the rate expected due to conventional muons alone.

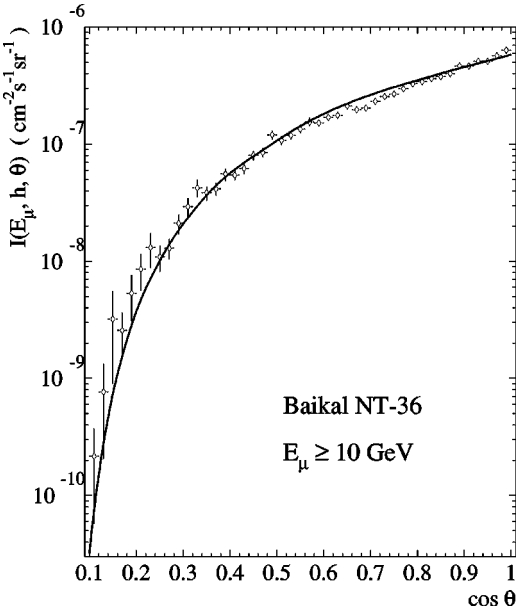

FIG. 3. Zenith angle distribution of the muon flux underwater measured by Baikal NT-36 [16].

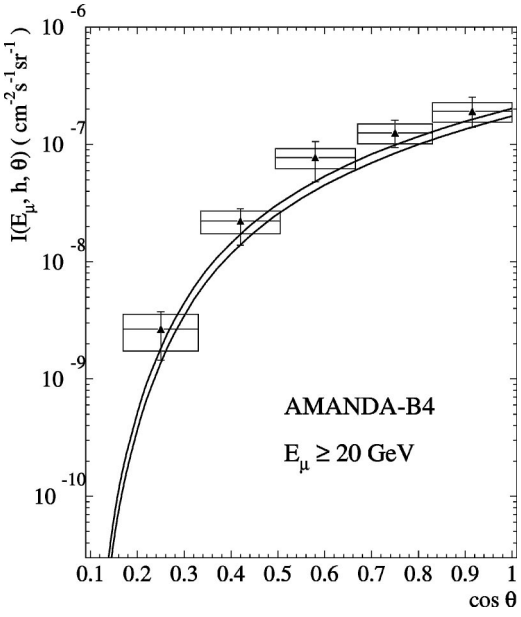

FIG. 4. Zenith angle distributions of the muon flux underwater measured with the AMANDA-B4 [17].

There is no intersection of the PQCD-2 line at $h=1.15$ km up to $\theta \sim 85°$. The intersection point shifts to smaller zenith angles with increasing depth. For a depth of 2 km (nearly the AMANDA depth) it is possible to observe prompt muon fluxes that would be expected with the PQCD-2 at not too large angles ($\sim 70°$). It should be mentioned that the underwater prompt muon flux will be distorted in a large zenith angle region because the angle isotropy approximation considered for the predictions of the PQCD models is valid only at $\theta \lesssim 70°$ and $E_\mu \lesssim 10^3$ TeV.

The depth dependence of the muon flux underwater at zenith angle of $\sim 78°$ (Fig. 6) indicates that in the case of the PQCD-1 one can observe the doubling of the muon flux at the Baikal depth of 1.15 km for $E_\mu \geqslant 100$ TeV. At a depth

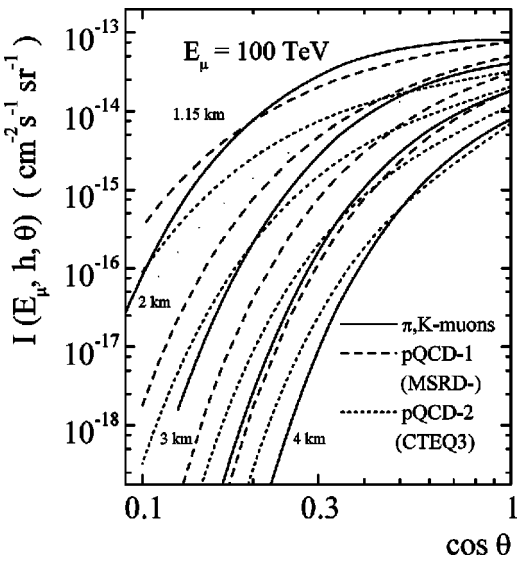

FIG. 5. Fluxes of muons above 100 TeV at water depth $h=1.15$, 2, 3, 4 km (from top to bottom) as a function of cosine of the zenith angle.

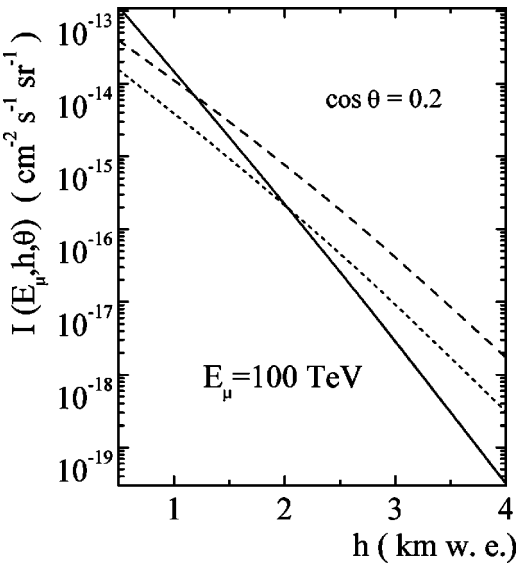

FIG. 6. The muon flux underwater against depth at $\cos\theta=0.2$. The contributions shown are the conventional muons (solid) and the prompt muons due to the PQCD-1 (dashed) and the PQCD-2 model (dotted).

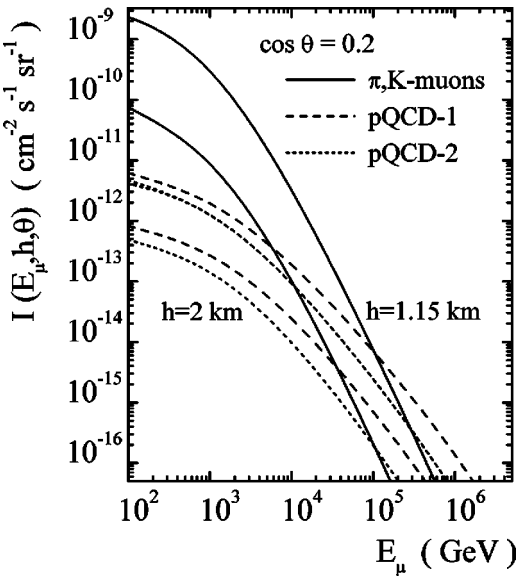

FIG. 7. Integral muon spectra underwater at zenith angle $\theta=78.5°$ at a depth of 1.15 km (upper) and of 2 km (lower). The contributions shown are the conventional muons (solid) and the prompt muons (dashed and dotted).

~ 2 km the same takes place even with the lesser prompt muon flux predicted with the PQCD-2 model.

Figure 7 shows muon integral energy spectra at a depth $h=1.15$ km (Baikal) and 2 km (AMANDA) and for $\cos\theta=0.2$ ($\theta\simeq 78.5°$). Also presented are the predictions of the prompt muon flux issued from the PQCD-1 (dashed) and PQCD-2 (dotted). The crossing energies $E_\mu^c(\theta)$ at the AMANDA depth are less than the ones at the Baikal depth by a factor of ~ 3. In particular, the PQCD-1 model gives $E_\mu^c(\theta\simeq 78.5°)\approx 30$ TeV at $h=2$ km and $E_\mu^c(78.5°)\approx 100$ TeV at a depth of 1.15 km. The same quantity calculated with PQCD-2 is 100 and 250 TeV, respectively.

One can see (Fig. 7) that the AMANDA depth (~ 2 km) gives, in a sense, the definite advantage in comparison with the Baikal one. Indeed, in the former case the assumed threshold energy is less, the muon flux difference between the PQCD-1 model and the PQCD-2 one is larger (up to two orders of magnitude), and the expected event rate remains approximately equal to the rate at the Baikal depth.

It should be pointed out that muon residual energies below ~ 10 TeV and zenith angle $\theta\lesssim 75°$ would be available (see Ref. [10] for a discussion), in the above context, in future high-energy muon experiments with the NESTOR deep-sea detector [32] which is expected to deploy at a depth of about 4 km.

IV. SUMMARY

Energy spectra and zenith angle distributions of the atmospheric muons at high energies have been calculated for the depths from 1 to 4 km that correspond to the depths of operation of large underwater neutrino telescopes. The estimation of the prompt muon contribution performed with the PQCD-1,2 shows that the crossing energy E_μ^c above which the prompt muon flux becomes dominant over the conventional one, is within the range of $\sim 200-\sim 500$ TeV at sea-level, depending on the choice of the parton distribution functions. For the flux underwater at a zenith angle $\sim 78°$, the PQCD-1 model leads to the value $E_\mu^c\simeq 30$ TeV ($h=2$ km) and $E_\mu^c\simeq 100$ TeV ($h=1.15$ km). The corresponding crossing energies for the PQCD-2 model are $E_\mu^c\simeq 100$ and $E_\mu^c\simeq 250$ TeV.

The absolute value of the muon flux underwater around E_μ^c depends on the charm production model. This circumstance enables, in principle, bounds to be put on the charm production cross section based on measurements of zenith angle distributions of the muon flux at high energies. In particular, PDF sets under discussion, the MRSD- and the CTEQ3, differ in the small-x behavior of the gluon distribution: $xg(x)\sim x^{-\lambda}$, where $\lambda\simeq 0.29$–0.35 for the CTEQ3 against $\lambda=0.5$ for the MRSD- set. (See Ref. [14] for the λ dependence of the sea-level prompt muon flux.) These PDF's yield inclusive cross sections of charmed particles produced in nucleon-air collisions and charm production cross sections that diverge rapidly from each other with increasing energy. For muon energies above 100 TeV and for $\cos\theta=0.2$ these differences lead to the fact that prompt muon flux predicted with the PQCD-1 exceeds the flux arising from the PQCD-2 model by a factor of about 4 at $h=1.15$ km or about 5 at $h=2$ km.

In conclusion we outline three probable ways for solving of the prompt muon problem in the underwater experiments. First, one can measure zenith angle dependence of the muon flux in the energy region of 50–100 TeV (see Fig. 5): the expected event rate with the Baikal NT-200 is about 200–300 per year per steradian, supposing that the effective area of NT-200 is 10^4 m^2 for $E_\mu\geqslant 100$ TeV [33].

Second, the flux with muon energies $E_\mu\geqslant 100$ TeV measured as a function of depth (say, in depth region about 0.8–1.2 km) at a given zenith angle ($\sim 78°$), could enable the charm production models to be discriminated (see Fig. 6) at

the event rate level of about 200 per year per steradian.

And last, one can attempt to extract information on the prompt muon flux underwater from muon integral spectra being measured at a given depth and at a given zenith angle (Fig. 7). In this case the event rate is a factor 7 less than in the previous one (with the NT-200 capabilities). It should be pointed out that the AMANDA depth of ~ 2 km provides some advantage: the threshold energy is less, the muon flux difference between the PQCD-1 model prediction and the PQCD-2 one is greater, and the expected event rate remains approximately equal to that at the Baikal depth.

ACKNOWLEDGMENTS

We thank V. A. Naumov for helpful discussions and comments and S. Hundertmark and C. Spiering for kindly providing the table data on the muon zenith-angle distribution and the depth-intensity relation measured in the AMANDA-B4 experiment. This work is supported in part by the Ministry of Education of the Russian Federation under Grant No. 015.02.01.04 (the Program ''Universities of Russia-Basic Researches'').

[1] L. V. Volkova and G. T. Zatsepin, Yad. Fiz. **37**, 353 (1983) [Sov. J. Nucl. Phys. **37**, 212 (1983)]; Izv. Akad. Nauk SSSR, Ser. Fiz. **49**, 1386 (1985).

[2] J. W. Elbert, T. K. Gaisser, and T. Stanev, Phys. Rev. D **27**, 1448 (1983).

[3] E. V. Bugaev, V. A. Naumov, and S. I. Sinegovsky, Yad. Fiz. **41**, 383 (1985) [Sov. J. Nucl. Phys. **41**, 245 (1985)].

[4] H. Inazawa, K. Kobayakawa, and T. Kitamura, J. Phys. G **12**, 59 (1986).

[5] L. V. Volkova, W. Fulgione, P. Galeotti, and O. Saavedra, Nuovo Cimento Soc. Ital. Fis., C **10**, 465 (1987).

[6] E. V. Bugaev, V. A. Naumov, S. I. Sinegovsky, and E. S. Zaslavskaya, Nuovo Cimento Soc. Ital. Fis., C **12**, 41 (1989), and references therein; E. V. Bugaev, V. A. Naumov, S. I. Sinegovsky, and E. S. Zaslavskaya, Izv. Akad. Nauk SSSR, Ser. Fiz. **53**, 342 (1989) [Bull. Acad. Sci. USSR, Phys. Ser. **53**, 135 (1989)].

[7] M. Thunman, G. Ingelman, and P. Gondolo, Astropart. Phys. **5**, 309 (1996).

[8] E. V. Bugaev, A. Misaki, V. A. Naumov *et al.*, Phys. Rev. D **58**, 054001 (1998).

[9] L. Pasquali, M. H. Reno, and I. Sarcevic, Phys. Rev. D **59**, 034020 (1999).

[10] A. Misaki *et al.*, in Proceedings of the 26th International Cosmic Ray Conference, Salt Lake City, Utah, 1999, edited by D. Kieda, M. Salamon, and B. Dingus, Vol. 2, p. 139 (HE 3.2.24), hep-ph/9905399; V. A. Naumov, T. S. Sinegovskaya, and S. I. Sinegovsky, Yad. Fiz. **63**, 2016 (2000) [Phys. At. Nucl. **63**, 1923 (2000)].

[11] G. Gelmini, P. Gondolo, and G. Varieschi, Phys. Rev. D **61**, 036005 (2000); **61**, 056011 (2000).

[12] A. D. Martin, W. J. Stirling, and R. G. Roberts, Phys. Rev. D **47**, 867 (1993); Phys. Lett. B **306**, 145 (1993).

[13] H. L. Lai *et al.*, Phys. Rev. D **51**, 4763 (1995).

[14] G. Gelmini, P. Gondolo, and G. Varieschi, Phys. Rev. D **63**, 036006 (2001).

[15] A. B. Kaidalov and O. I. Piskunova, Yad. Fiz. **43**, 1545 (1986) [Sov. J. Nucl. Phys. **43**, 994 (1986)]; Z. Phys. C **30**, 145 (1986); O. I. Piskunova, Yad. Fiz. **56**, 176 (1993) [Phys. At. Nucl. **56**, 1094 (1993)].

[16] Baikal Collaboration, I. A. Belolaptikov *et al.*, Astropart. Phys. **7**, 263 (1997).

[17] AMANDA Collaboration, E. Andres *et al.*, Astropart. Phys. **13**, 1 (2000).

[18] A. N. Vall, V. A. Naumov, and S. I. Sinegovsky, Yad. Fiz. **44**, 1240 (1986) [Sov. J. Nucl. Phys. **44**, 806 (1986)].

[19] V. A. Naumov, T. S. Sinegovskaya, and S. I. Sinegovsky, Nuovo Cimento A **111**, 129 (1998).

[20] S. I. Nikol'sky, J. N. Stamenov, and S. Z. Ushev, Zh. Éksp. Teor. Fiz. **87**, 18 (1984) [Sov. Phys. JETP **60**, 10 (1984)].

[21] B. C. Rastin, J. Phys. G **10**, 1609 (1984).

[22] S. Matsuno *et al.*, Phys. Rev. D **29**, 1 (1984).

[23] G. T. Zatsepin *et al.*, Izv. Ross. Akad. Nauk, Ser. Fiz. **58**, 119 (1994) [Bull. Acad. Sci. USSR, Phys. Ser. **58**, 2050 (1994)].

[24] W. Rhode, Nucl. Phys. B (Proc. Suppl.) **35**, 250 (1994).

[25] LVD Collaboration, M. Aglietta *et al.*, Phys. Rev. D **58**, 092005 (1998).

[26] F. F. Khalchukov *et al.*, in Proceedings of the 19th International Cosmic Ray Conference, La Jolla, California, 1985, edited by F. C. Jones *et al.*, Vol. 8, p. 12.

[27] V. N. Bakatanov *et al.*, Yad. Fiz. **55**, 2107 (1992) [Sov. J. Nucl. Phys. **55**, 1169 (1992)].

[28] MACRO Collaboration, M. Ambrosio *et al.*, Phys. Rev. D **52**, 3793 (1995).

[29] T. S. Sinegovskaya, in *Proceedings of the Second Baikal School on Fundamental Physics ''Interaction of Radiation and Fields with Matter,''* Irkutsk, Russia, 1999, edited by Yu. N. Denisyuk and A. N. Malov (Irkutsk State University, Irkutsk, 1999), Vol. 2, p. 598 (in Russian).

[30] LVD Collaboration, M. Aglietta *et al.*, Phys. Rev. D **60**, 112001 (1999).

[31] V. A. Naumov, S. I. Sinegovsky, and E. V. Bugaev, Yad. Fiz. **57**, 439 (1994) [Phys. At. Nucl. **57**, 412 (1994)]; hep-ph/9301263.

[32] NESTOR Collaboration, B. Monteleoni, in *Proceedings of the Baikal School on Fundamental Physics ''Astrophysics and Microworld Physics,''* Irkutsk, Russia, 1998, edited by V. A. Naumov, Yu. V. Parfenov, and S. I. Sinegovsky (Irkutsk State University, Irkutsk, 1998), p. 105; NESTOR Collaboration, E. G. Anassontzis *et al.*, Nucl. Phys. B (Proc. Suppl.) **66**, 247 (1998); NESTOR Collaboration, S. Bottai, in Proceedings of the 26th International Cosmic Ray Conference (Ref. [10]), Vol. 2, p. 456 (HE 6.3.08).

[33] Baikal Collaboration, V. A. Balkanov *et al.*, in Proceedings of the 26th International Cosmic Ray Conference (Ref. [10]), Vol. 2, p. 217 (HE 4.2.04).